

## Improving experimental procedures for assessing electrical properties of advanced liquid crystal materials

O. V. Kovalchuk, Anatoliy Glushchenko & Yuriy Garbovskiy

To cite this article: O. V. Kovalchuk, Anatoliy Glushchenko & Yuriy Garbovskiy (2023) Improving experimental procedures for assessing electrical properties of advanced liquid crystal materials, *Liquid Crystals*, 50:1, 140-148, DOI: [10.1080/02678292.2022.2114027](https://doi.org/10.1080/02678292.2022.2114027)

To link to this article: <https://doi.org/10.1080/02678292.2022.2114027>



Published online: 26 Aug 2022.



Submit your article to this journal [↗](#)



View related articles [↗](#)



View Crossmark data [↗](#)

## Improving experimental procedures for assessing electrical properties of advanced liquid crystal materials

O. V. Kovalchuk<sup>a,b,c</sup>, Anatoliy Glushchenko<sup>d\*</sup> and Yuriy Garbovskiy<sup>e†</sup>

<sup>a</sup>Department of Applied Physics and Higher Mathematics, Kyiv National University of Technologies and Design, Kyiv, Ukraine; <sup>b</sup>Department of General Physics and Modeling of Physical Processes, National Technical University of Ukraine 'Igor Sikorsky Kyiv Polytechnic Institute', Kyiv, Ukraine; <sup>c</sup>Institute of Physics, NAS of Ukraine, Kyiv, Ukraine; <sup>d</sup>Department of Physics, University of Colorado Colorado Springs, Colorado Springs, CO, USA; <sup>e</sup>Department of Physics and Engineering Physics, Central Connecticut State University, New Britain, CT, USA

### ABSTRACT

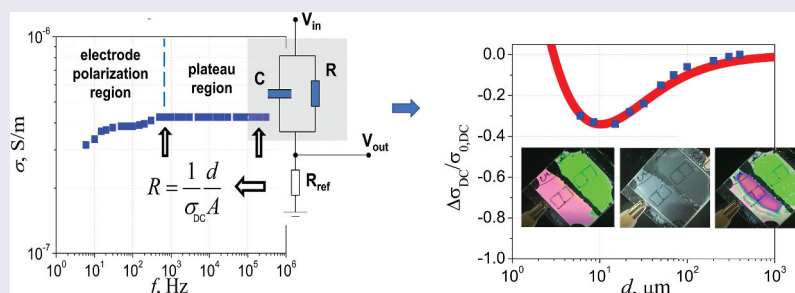
Electrical measurements of liquid crystals are a standard part of their material characterisation. Typically, such measurements are carried out using a sandwich-like cell of a single thickness. In this paper, we show that interactions between ions and substrates of a liquid crystal cell result in the dependence of the direct current electrical conductivity of liquid crystal materials on the cell thickness. The obtained experimental results combined with modelling point to the existence of ions of several types and to the competition between ion-releasing and ion-trapping processes in liquid crystal cells. We also propose to use a multi-electrode twin-cell that allows the visualisation of the electric field screening effect in liquid crystals and its mitigation by means of ferroelectric nanoparticles.

### ARTICLE HISTORY

Received 24 June 2022

### KEYWORDS

Liquid crystals; ions; electrical conductivity; ionic contamination; nanoparticles



### Introduction

Display and non-display applications of liquid crystals continue to expand and evolve [1]. In addition to the large-area liquid crystal displays (LCD) [2,3] and miniature high-resolution displays for AR/VR [4,5], liquid crystals become a material of choice for tunable optical devices including waveguides [6], lenses [7], spatial light modulators [8], filters and waveplates [9] and diffractive elements [10], to name a few. Liquid crystal materials are also very promising for the design and fabrication of reconfigurable meta- and plasmonic devices [11,12], and numerous devices operating at microwave frequencies (phase shifters, tunable filters, resonators, and antennas) [13,14]. Last but not least, modern demands for smart windows revitalised the field of liquid crystal shutters and privacy windows [15–17].

The reorientation of a liquid crystal director under the action of the applied electric field enables the tunability of the aforementioned devices [18]. This electric field-induced orientation effect can be altered by the ions normally present in molecular liquid crystals in small quantities [19–21]. Ions in liquid crystals result in finite values of their direct current (DC) electrical conductivity [19–21]. Along with other relevant material parameters (optical birefringence, dielectric anisotropy, elastic constants, rotational viscosity, etc.), the value of the DC electrical conductivity determines the suitability of liquid crystal materials for a chosen application [19–22]. That is why since the release of commercial liquid crystal devices back in the 1960s, electrical measurements of liquid crystals became a standard part of their material characterisation [22]. As a result, many papers improving our understanding

**CONTACT** Yuriy Garbovskiy  [ygarbovskiy@ccsu.edu](mailto:ygarbovskiy@ccsu.edu)

\*Formerly at the Institute of Physics, Kyiv, Ukraine (1995–2000). Received his PhD in Physics from the Institute of Physics, Kyiv, Ukraine, in 1997.

†Formerly at the Institute of Physics, Kyiv, Ukraine (2003–2009). Received his PhD in Physics from the Institute of Physics, Kyiv, Ukraine, in 2007.

of ions and ionic effects in liquid crystals have been published [21,23–28; and references therein].

Standard experimental techniques for measuring the basic electrical parameters (DC conductivity, charge mobility and ion density) of liquid crystal materials include transient current measurements [23–25] and dielectric and impedance spectroscopy [26–29]. In addition, experimental methods that are very common in industry include the voltage-holding ratio [30] and residual DC voltage measurements [30,31] and flicker minimisation technique [30–32]. As a rule, electrical measurements of liquid crystal materials are carried out using a sandwich-like cell of a single thickness. Only a very limited number of papers report experimental results obtained using several cells of different thicknesses [26,33–36]. Papers [26,29,33–36] unambiguously indicate that the measured values of the concentration of ions and DC electrical conductivity depend on the cell thickness. Possible types of such a dependence were recently modelled in a few papers [37–40]. At the same time, there are still no systematic studies combining both experiments and modelling of the dependence of the DC electrical conductivity on the cell thickness. The present paper aims at filling this gap.

Another objective of the present paper is related to the visualisation of the electric field screening effect in liquid crystals. This effect is caused by ions in liquid crystals when an applied electric field separates positive and negative ions, thus creating a screening electric field due to the separated ions [20,21,41]. The screening electric field acts against the applied electric field, and it does not disappear immediately once the applied field is turned off. The screening effect can result in many undesirable outcomes including image sticking, image flickering, reduced voltage-holding ratio and overall slow response of a liquid crystal device [20,21]. The origin of this effect is well documented in the literature [20,21,41–45], and time-dependent capacitance [41,42] and electro-optical measurements [43–45] were carried out to study the effect. In this paper, we propose to combine electro-optical measurements with a digital imaging that allows the visualisation of the screening effect in liquid crystals. We also propose to use a multi-electrode twin-cell for a visual observation of the ion screening effect and its mitigation by means of ferroelectric nanoparticles.

## Experimental methods and materials

Dielectric spectroscopy is a versatile technique to study dielectric and electrical properties of a wide range of materials including liquid crystals [29,46]. In this paper, we adopted an oscilloscopic method [47,48] to measure

a frequency-dependent electrical conductivity of nematic liquid crystals as a function of cell thickness. Within a certain frequency range (typically,  $10^3$ – $10^5$  Hz), the sandwich-like cell can be modelled as an ideal capacitor and resistor combined in parallel as shown in Figure 1. By measuring an applied voltage  $V_{in}$ , and a voltage drop  $V_{out}$  across a reference resistor of resistance  $R_{ref}$  using an oscilloscope, both capacitance  $C$  and resistance  $R$  of the studied liquid crystal cell can be found [47,48] (Figure 1). As a result, frequency-dependent dielectric permittivity  $\epsilon$  and conductivity  $\sigma$  can be obtained. Figure 1 shows a typical dependence of dielectric permittivity  $\epsilon$  and electrical conductivity  $\sigma$  on frequency  $f$  measured using nematic liquid crystals 6CB. In this paper, we focus on the DC electrical conductivity  $\sigma_{DC}$  of liquid crystals (it corresponds to a plateau region ( $10^3$ – $10^5$  Hz) of the  $\sigma(f)$  dependence in Figure 1).

Sandwich-like cells of known thickness were filled with commercially available nematic liquid crystals (BL055 [49], ZhK1282 [50], MJ961180 [51]). The cell thickness was controlled using spacers. Indium-tin oxide (ITO) substrates were covered with rubbed thin polyimide films to impose planar boundary conditions.

Electro-optical measurements were performed by placing a liquid crystal cell in between two crossed polarisers. A DC voltage (15 V) was applied across the cell, and an intensity of a He-Ne laser beam (632.8 nm) was measured using a photodiode. For digital imaging experiments, a recently designed twin-cell was used [52,53]. The twin-cell was placed in between two crossed polarisers, a laser was replaced with a light box (a conventional incandescent bulb was used as a source of white light), and a digital camera was utilised to acquire digital images.

## Experimental results and discussion

### DC electrical conductivity and its dependence on the cell thickness

Several ionic processes can contribute to the dependence of the DC electrical conductivity of liquid crystals on the cell thickness. Ions already present in liquid crystals can be captured by the substrates of a liquid crystal cell. Some fraction of captured ions can be released back into the bulk until equilibrium is reached. Such ionic processes result in a decrease in the DC electrical conductivity. However, very often, substrates can enrich liquid crystals with new ions that were trapped on substrates of an empty cell before it was filled with liquid crystals. This release of ions by substrates results in an increase in the DC electrical conductivity. In any real situation, we can expect the

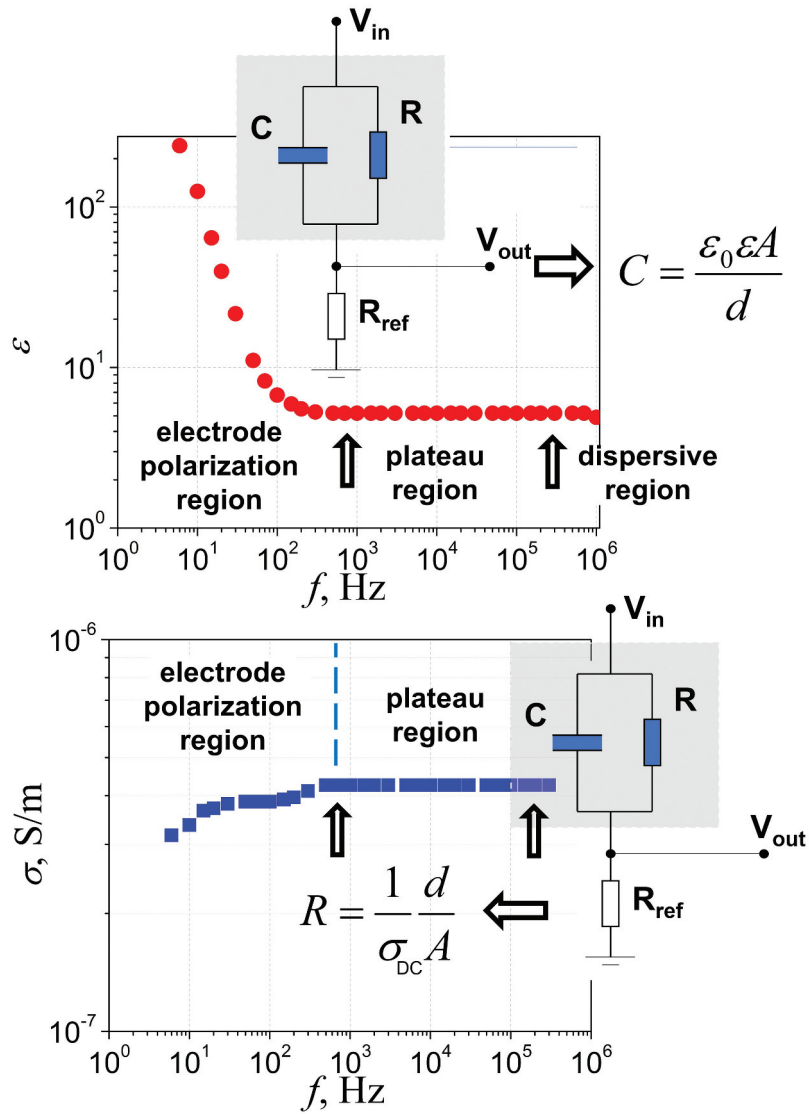


**Figure 1.** (Colour online) Frequency-dependent dielectric permittivity  $\varepsilon$  and electrical conductivity  $\sigma$  of nematic liquid crystals measured by means of an oscilloscopic technique. In the plateau region ( $10^3$ – $10^5$  Hz), a liquid crystal cell is modelled as a capacitor of a capacitance  $C$  and a resistor of resistance  $R$  combined in parallel.

competition between ion-capturing and ion-releasing processes leading to the dependence of the DC electrical conductivity on the cell thickness. To show experimentally that this effect is very common, three types of nematic liquid crystals were tested. To compare different materials and the strength of this dependence, we plotted a relative change in the DC electrical conductivity defined by Equation (1):

$$\frac{\Delta\sigma_{DC}}{\sigma_{0DC}} = \frac{\sigma_{DC} - \sigma_{0DC}}{\sigma_{0DC}} \quad (1)$$

where  $\sigma_{0DC}$  is the initial DC electrical conductivity of liquid crystals (it is not affected by ion-capturing and ion-releasing processes; experimentally measurements are taken immediately after filling the cell with liquid crystals) and  $\sigma_{DC}$  is the steady-state value of the DC

electrical conductivity (measurements are taken after waiting for sufficiently long time, typically 1–2 days).

The results shown in Figures 2–4 illustrate the dependence of the DC electrical conductivity on the cell thickness.

Monotonous dependence of the relative change in the DC electrical conductivity  $\frac{\Delta\sigma_{DC}}{\sigma_{0DC}}$  on the cell thickness  $d$  was found for nematic liquid crystal BL055 (Figure 2).

At the same time, nematic liquid crystals ZhK1282 and MJ961180 exhibit non-monotonous dependence  $\frac{\Delta\sigma_{DC}}{\sigma_{0DC}}$  vs.  $d$  (Figures 3 and 4).

Figures 2–4 share one important feature. The relative change in the DC electrical conductivity is negative for thin cells and becomes zero for thick cells. This behaviour can be explained in the following way. In the case of thin cells, the ion-capturing effect caused by the substrates is

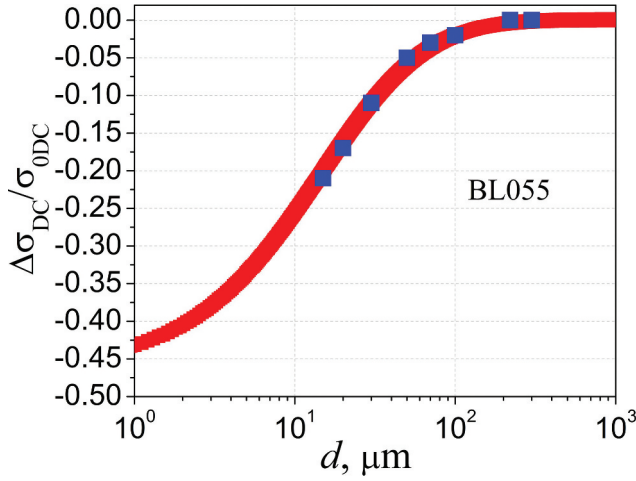


**Figure 2.** (Colour online) The dependence of a relative change in the DC electrical conductivity of nematic liquid crystals BL055 on the cell thickness. Squares are experimental data points. Solid curve is generated by applying Equations (1)–(4).

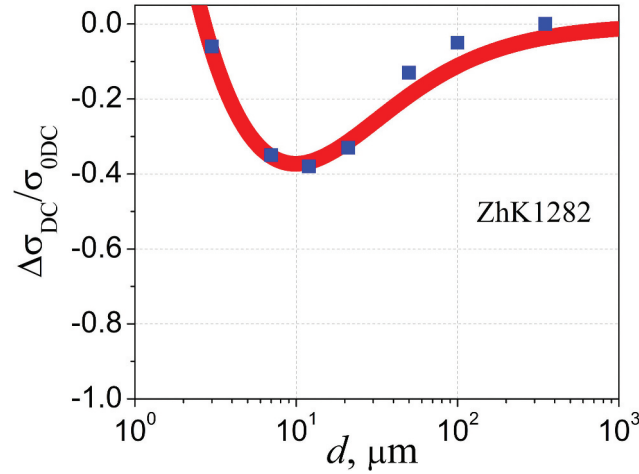


**Figure 3.** (Colour online) The dependence of a relative change in the DC electrical conductivity of nematic liquid crystals ZhK1282 on the cell thickness. Squares are experimental data points. Solid curve is generated by applying Equations (1)–(4).

a dominant factor governing the value of the DC electrical conductivity. As a result,  $\Delta\sigma_{DC}$  is negative. The effect of this substrates-induced ion-capturing process becomes insignificant for thicker cells ( $\Delta\sigma_{DC} \rightarrow 0$ ).

By applying a recently developed elementary model of ion generation and ion capturing in liquid crystal cells [37–40], additional information about ionic processes in liquid crystals can be obtained. Assuming two types of fully ionised ionic species, the DC electrical conductivity  $\sigma_{DC}$  of liquid crystals is given by Equation (2):

$$\sigma_{DC} = \sum_i q_i \mu_i n_i \quad (2)$$

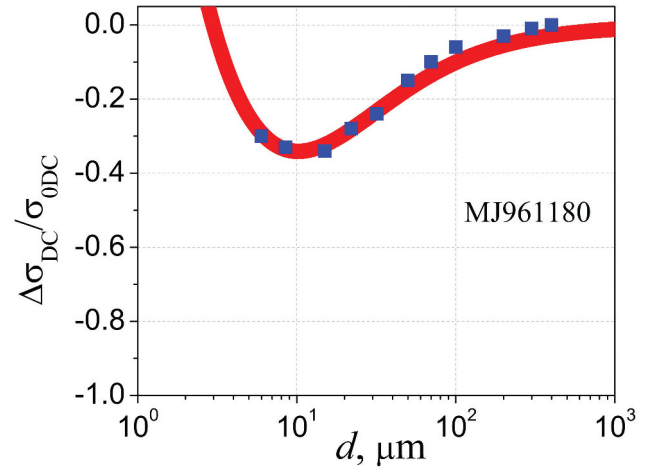


**Figure 4.** (Colour online) The dependence of a relative change in the DC electrical conductivity of nematic liquid crystals MJ961180 on the cell thickness. Squares are experimental data points. Solid curve is generated by applying Equations (1)–(4).

where  $q_i = |e| = 1.6 \times 10^{-19} C$  ( $i = 1, 2$ ),  $n_i^+ = n_i^- = n_i$  is the volume concentration of ions of type  $i$  ( $i = 1, 2$ ),  $\mu_i = \mu_i^+ + \mu_i^-$  is the effective ion mobility of type  $i$  ( $i = 1, 2$ ). Index  $i = 1$  stands for fully dissociated ionic species present in liquid crystals prior to filling an empty cell, and index  $i = 2$  denotes ions originated from the substrates of a cell. Interactions between ions of type  $i$  and substrates are described by rate Equation (3):

$$\frac{dn_i}{dt} = -k_{Si}^{a\pm} n_i \frac{\sigma_{Si}}{d} (1 - \Theta_{S1}^{\pm} - \Theta_{S2}^{\pm}) + k_{Si}^{d\pm} \frac{\sigma_{Si}}{d} \Theta_{Si}^{\pm} \quad (3)$$

In Equation (3), the time rate of ion capturing and ion releasing processes is described by the parameters  $k_{Si}^{a\pm}$  and  $k_{Si}^{d\pm}$ . Quantities  $\Theta_{Si}^{\pm}$  stand for the fractional surface coverage of substrates by the  $i$ -th ions ( $i = 1, 2$ );  $\sigma_{Si}$  is the surface density of all surface sites on two substrates; and  $d$  is the cell thickness. Because both ion capturing (the first term of Equation (3)) and ion releasing (the second term of Equation (3)) processes depend on the cell thickness  $d$ , the bulk concentration of mobile ions is also thickness-dependent.

The conservation of the total number of ions of the  $i$ -th type can be written as Equation (4):

$$n_{0i} + \frac{\sigma_{Si}}{d} v_{Si} = n_i + \frac{\sigma_{Si}}{d} \Theta_{Si}^{\pm} \quad (4)$$

where  $n_{0i}$  is the initial concentration of ions of the  $i$ th type in liquid crystals and  $v_{Si}$  is the contamination factor of substrates [37–40].

The results of modelling using Equations (1)–(4) are also shown in Figures 2–4 (solid curves). The system of Equations (3) and (4) was solved to find steady state

values of  $n_1$  and  $n_2$ . Having  $n_1$  and  $n_2$  both initial  $\sigma_{0DC}$  and steady state  $\sigma_{DC}$  DC electrical conductivity was computed by applying Equation (2). Finally, the obtained values of  $\sigma_{0DC}$  and  $\sigma_{DC}$  were used to find the dependence of the ratio  $\frac{\sigma_{DC}-\sigma_{0DC}}{\sigma_{0DC}}$  on the cell thickness (Equation (1)). Table 1 compiles the values of the physical parameters used to generate the solid curves shown in Figures 2–4. Index ‘1’ refers to ions already present in liquid crystals (the contamination factor is zero,  $v_{S1} = 0$ ), and index ‘2’ stands for ions originated from the substrates (the contamination factor is nonzero but still small,  $v_{S2} \approx 10^{-3}$ ). A nonzero contamination factor means that substrates of a liquid crystal cells are contaminated with ions prior to filling them with liquid crystal materials.

Figures 2–4 indicate that the evaluation of the DC electrical conductivity of liquid crystal materials is not a simple and straightforward process. In general, the obtained value of the DC conductivity depends on the cell thickness and on the type of substrates used in experiments. This experimental fact should be taken into consideration by scientists and engineers involved in the design and characterisation of new liquid crystal materials and devices.

Because Equations (3) and (4) are essentially the Langmuir adsorption model developed for neutral particles [29], it is important to comment on its applicability to describe the adsorption of ions in liquid crystal cells. Even though the Langmuir model was developed to analyse the adsorption of neutral particles, under certain conditions this model can also be applied to the adsorption of ions in liquid crystals as was recently discussed in papers [37–40]. These conditions are fulfilled in the case of molecular liquid crystals characterised by relatively low concentrations of ions ( $10^{18}$ – $10^{20} \text{ m}^{-3}$ ) and small values of the surface coverage of the alignment layers ( $10^{-3}$ – $10^{-4}$ ) [37–40]. Such conditions also allow to assume an independence of the ion mobility of the ion bulk density and the applicability of

Equation (2). As was discussed in [37], the parameter  $\sigma_{Si}$  can be estimated as an inverse square of the average size  $r = 1 - 10 \text{ nm}$  of the organic macro-block corresponding to an adsorption site of the alignment layer (polyimide film) for an ion of a given size (in this case we can assume that the size of the ion is related to the size of the adsorption site). An order-of magnitude estimate for  $\sigma_{Si} \approx 1/r^2$  yields  $\sigma_{Si} \approx 10^{16} - 10^{18} \text{ m}^{-2}$  [37].

### Visualising the electric field screening effect in liquid crystals

Future progress of liquid crystal science and technology relies heavily on the development of advanced liquid crystal materials. A quite general approach involves the comparative analysis of the properties of the newly synthesised homologous series of liquid crystal materials [22] or liquid crystals doped with nanoparticles [21,54,55]. In the former case, the properties of a homologous series are tested against the properties of a reference sample. In the latter case, the properties of liquid crystals doped with nanomaterials are compared with the properties of undoped liquid crystals. If electrical characterisation of such materials should be performed, the dependence of the DC electrical conductivity on the cell thickness shown in Figures 2–4 must be taken into consideration. Indeed, even for the same liquid crystal material, electrical measurements carried out using cells of different thickness yield different results (Figures 2–4). Existing experimental procedures of electrical characterisation of liquid crystals can be improved by using a multi-electrode twin-cell shown in Figure 5. A cell is divided into two identical (the same thickness and the same boundary conditions) regions separated by a polymer stripe. Depending on the experimental needs, 2-, 3- or 4-electrode configuration can be used (Figure 5(c)). Using a twin-cell placed between two crossed polarisers as shown in Figure 5(a), in addition to performing standard electrical measurements, it is also possible to visualise an electric field screening effect and its mitigation by means of ferroelectric nanoparticles (Figure 5(b)).

In Figure 5(b), one-half of a twin-cell is filled with pure (undoped) nematic liquid crystals 5CB (it is denoted as LC), and one-half of the same cell is filled with nematic liquid crystals doped with ferroelectric nanoparticles  $\text{Sn}_2\text{P}_2\text{S}_6$  (this region of the cell is denoted as LC/FNP). The description of the preparation of ferroelectric nanoparticles and liquid crystal colloids was already reported in papers [52,53]. The substrates of the cell are spin-coated with a polyimide polymer to provide a homogeneous alignment of liquid crystals.

**Table 1.** Physical parameters and their values.

Physical parameter	Liquid crystal materials		
	BL055	ZhK-1282	MJ961180
$n_{01}, \text{m}^{-3}$	$5 \times 10^{18}$	$2.6 \times 10^{18}$	$1.5 \times 10^{18}$
$n_{02}, \text{m}^{-3}$	0	0	0
$K_1 = \frac{k_{31}^{\sigma+}}{k_{31}^{\sigma-}}, \text{m}^3$	$1.5 \times 10^{-23}$	$4.5 \times 10^{-24}$	$4 \times 10^{-24}$
$K_2 = \frac{k_{32}^{\sigma+}}{k_{32}^{\sigma-}}, \text{m}^3$	$1.75 \times 10^{-22}$	$1 \times 10^{-22}$	$5 \times 10^{-24}$
$\sigma_{S1}, \text{m}^{-2}$	$1.5 \times 10^{18}$	$3.5 \times 10^{18}$	$3.6 \times 10^{18}$
$\sigma_{S2}, \text{m}^{-2}$	$2.5 \times 10^{17}$	$0.15 \times 10^{16}$	$0.75 \times 10^{16}$
$v_{S1}$	0	0	0
$v_{S2}$	$4.7 \times 10^{-3}$	$5.6 \times 10^{-3}$	$2.5 \times 10^{-3}$
$\frac{\mu_2}{\mu_1}$	0.1	0.75	0.2

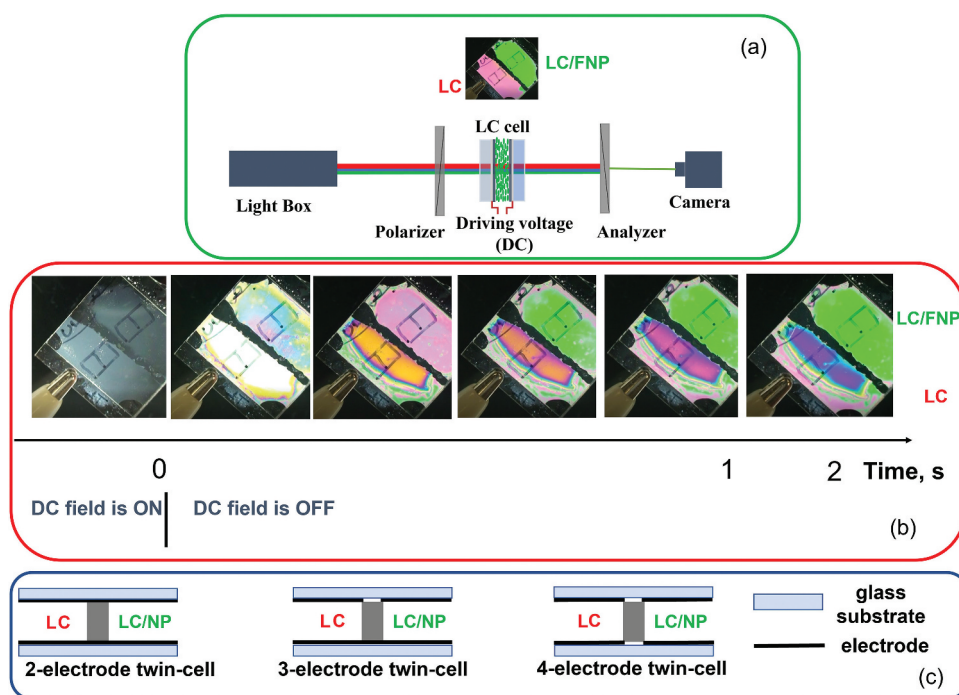


**Figure 5.** (Colour online) Twin-Cells for the visualisation of the ion screening effects. (a) Experimental set-up. (b) A series of snapshots taken after the DC electric field was turned off (electrodes are short-circuited). (c) A multi-electrode twin-cell.

A constant voltage (15 V) is applied across the cell. As a result, the liquid crystal director is reoriented from a planar to homeotropic configuration and white light does not pass through the twin-cell (Figure 5(b), ‘DC field is ON’). Once the applied DC field is turned off, liquid crystals reorient back to their initial planar state. A series of snapshots are taken by a digital camera. It allows for a direct visualisation of the director reorientation process (Figure 5(b)). In the case of a pure liquid crystal, the reorientation process is very slow, whereas the reorientation of liquid crystals doped with ferroelectric nanoparticles takes more than one order of magnitude shorter time, in agreement with the well-known Equation (5):

$$t_{off} = \frac{\gamma d^2}{\pi^2 K_{11}} \quad (5)$$

where  $\gamma$  is the rotational viscosity,  $d$  is the cell thickness, and  $K_{11}$  is an elastic constant [18].

In the case of undoped liquid crystals 5CB, much longer turn-off time is caused by the screening effect originated due to separated positive and negative ions in liquid crystals, as described in the introduction section of this paper. An in-depth discussion of this effect can be found in paper [41]. It is a well-known experimental fact that under certain conditions [56], ferroelectric nanoparticles can trap ions in liquid crystals [57–62]. This nanoparticle-induced ion-trapping process can mitigate the electric field screening effect by practically

eliminating it. As a result, the turn-off time of liquid crystals doped with ferroelectric nanoparticles is not affected by ions as can be seen in Figure 5(b). At the same time, the electric field screening effect is clearly observed in the case of undoped liquid crystals (Figure 5(b)). Thus, the experimental arrangement shown in Figure 5 allows for the visualisation of the electric field screening effect in nematic liquid crystals and its mitigation by means of nanoparticles.

Exact values of both turn-on and turn-off times of liquid crystals and liquid crystals doped with ferroelectric nanoparticles can be found by performing standard electro-optical measurements when a white light source in Figure 5(a) is replaced with a He-Ne laser, and a camera is replaced with a photodiode measuring the dependence of the intensity of the transmitted light  $I$  on time (Figure 6).

## Conclusion

Even though electrical measurements of liquid crystal materials were discussed in many papers, there is still plenty of room for improvements to existing experimental procedures. The substrates of a liquid crystal cell play a dual role. They can act as a source of ions because of their uncontrolled ionic contamination. This factor leads to the increase in the concentration of ions and DC electrical conductivity of liquid crystals [63,64]. The substrates can also capture ions thus resulting in the decrease

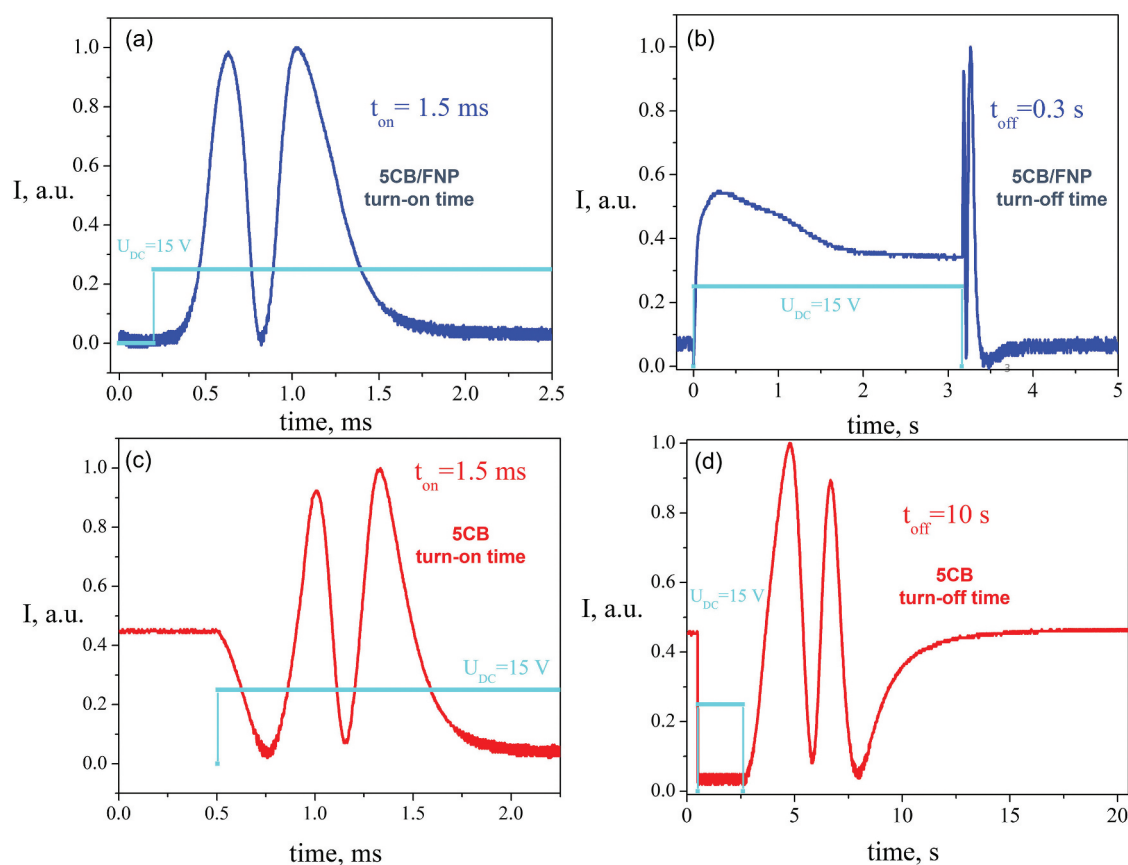


**Figure 6.** (Colour online) Time-dependent electro-optics (turn-on and turn-off time response) of doped with ferroelectric nanoparticles  $\text{Sn}_2\text{P}_2\text{S}_6$  (a,b) and undoped nematic liquid crystals (c,d) driven by a DC electric field.

in the concentration of ions and DC electrical conductivity [65,66]. In any real situation, the consequence of the competition between ion-capturing and ion-releasing processes is the dependence of the DC electrical conductivity on the cell thickness (Figures 2–4). As a result, the correct evaluation of the DC electrical conductivity of existing and new liquid crystal materials requires a series of measurements carried out using cells of different thicknesses. The DC electrical conductivity is strongly affected by interactions between ions and substrates if thin liquid crystal cells are studied. Because thin layers of liquid crystals are typically utilised for the design of many commercial products, this factor is very important at the stage of the material selection when the suitability of a liquid crystal material for a chosen application is considered. At the same time, the effect of ion-capturing and ion-releasing processes on the measured value of the DC electrical conductivity becomes insignificant for thicker cells (Figures 2–4).

If nanomaterials are used to modify the properties of liquid crystals, a multi-electrode twin-cell can be considered for electrical and electro-optical measurements (Figures 5 and 6). Such cells driven by a DC electric field

allow for a direct visualisation of the electric field screening effect. In addition, they simplify the correct comparison of the properties of plain and doped with nanoparticles liquid crystals, thus eliminating ambiguous conclusions and leading to a better understanding of the effects of nanomaterials on the properties of liquid crystals.

### Disclosure statement

No potential conflict of interest was reported by the author(s).

### Funding

This research was supported by the CSU—AAUP Faculty Research Grant.

### ORCID

O. V. Kovalchuk <http://orcid.org/0000-0002-9404-5853>  
 Anatoliy Glushchenko <http://orcid.org/0000-0001-6059-649X>  
 Yuriy Garbovskiy <http://orcid.org/0000-0003-3047-8761>

## References

- [1] Schenning APHJ, Crawford GP, Broer DJ, editors. Liquid crystal sensors. Boca Raton (FL): CRC Press, Taylor & Francis Group; 2018. p. 164.
- [2] Jones C. The fiftieth anniversary of the liquid crystal display. *Liq Cryst Today*. 2018;27(3):44–70.
- [3] Chen HW, Lee JH, Lin BY, et al. Liquid crystal display and organic light-emitting diode display: present status and future perspectives. *Light: Sci Appl*. 2018;7:17168.
- [4] Xiong J, Hsiang EL, He Z, et al. Augmented reality and virtual reality displays: emerging technologies and future perspectives. *Light: Sci Appl*. 2021;10(1):216.
- [5] Wang YJ, Lin YH. Liquid crystal technology for vergence-accommodation conflicts in augmented reality and virtual reality systems: a review. *Liq Cryst Rev*. 2021;9(1):35–64.
- [6] d'Alessandro A, Asquini R. Light propagation in confined nematic liquid crystals and device applications. *Appl Sci*. 2021;11(18):8713.
- [7] Lin YH, Wang YJ, Reshetnyak V. Liquid crystal lenses with tunable focal length. *Liq Cryst Rev*. 2017;5(2):111–143.
- [8] Otón JM, Otón E, Quintana Xand Geday MA. Liquid-crystal phase-only devices. *J Mol Liq*. 2018;267:469–483.
- [9] Abdulhalim I. Non-display bio-optic applications of liquid crystals. *Liq Cryst Today*. 2011;20(2):44–60.
- [10] Morris R, Jones C, Nagaraj M. Liquid crystal devices for beam steering applications. *Micromach*. 2021;12:247.
- [11] Lininger A, Zhu AY, Park JS, et al. Optical properties of metasurfaces infiltrated with liquid crystals. *Proc Natl Acad Sci*. 2020;117(34):202006336.
- [12] Jeng SC. Applications of Tamm plasmon-liquid crystal devices. *Liq Cryst*. 2020;47:1223–1231.
- [13] Camley R, Celinski Z, Garbovskiy Y, et al. Liquid crystals for signal processing applications in the microwave and millimeter wave frequency ranges. *Liq Cryst Rev*. 2018;6(1):17–52.
- [14] Jakoby R, Gaebler A, Weickmann C. Microwave liquid crystal enabling technology for electronically steerable antennas in SATCOM and 5G millimeter-wave systems. *Crystals*. 2020;10:514.
- [15] Geis MW, Bos PJ, Liberman V, et al. Broadband optical switch based on liquid crystal dynamic scattering. *Opt Express*. 2016;24(13):13812–13823.
- [16] Dabrowski R, Dziaduszek J, Bozетка J, et al. Fluorinated smectics – new liquid crystalline medium for smart windows and memory displays. *J Mol Liq*. 2017;267:415–427.
- [17] Castellón E, Levy D, editors. Smart windows based on liquid crystal dispersions. Weinheim (Germany): Wiley-VCH; chapter 5.4., Transparent conductive materials. 2018. p. 337–365.
- [18] Chigrinov VG. Liquid crystal devices: physics and applications. Boston (MA): Artech House; 1999.
- [19] Naemura S. Electrical properties of liquid crystal materials for display applications. *Mat Res Soc Symp Proc*. 1999;559:263–274.
- [20] Neyts K, Beunis F. Handbook of liquid crystals: physical properties and phase behavior of liquid crystals. Vol. 2. Germany: Wiley-VCH; 2014. Chapter 11, Ion transport in liquid crystals. p. 357–382.
- [21] Garbovskiy Y. Conventional and unconventional ionic phenomena in tunable soft materials made of liquid crystals and nanoparticles. *Nano Ex*. 2021;2(1):012004.
- [22] Goodby JW, Cowling SJ. Conception, discovery, invention, serendipity and consortia: cyanobiphenyls and beyond. *Crystals*. 2022;12:825.
- [23] Colpaert C, Maximus B, Meyere D. Adequate measuring techniques for ions in liquid crystal layers. *Liq Cryst*. 1996;21(1):133–142.
- [24] Vaxiviere J, Labroo B, Martinot-Lagarde P. Ion bump in the ferroelectric liquid crystal domains reversal current. *Mol Cryst Liq Cryst*. 1989;173:61–73.
- [25] Sugimura A, Matsui N, Takahashi Y, et al. Transient currents in nematic liquid crystals. *Phys Rev B*. 1991;43(10):8272–8276.
- [26] Khazimullin MV, Lebedev YA. Influence of dielectric layers on estimates of diffusion coefficients and concentrations of ions from impedance spectroscopy. *Phys Rev E*. 2019;100(6):062601.
- [27] Sawada A, TarumiKand Naemura S, Naemura S. Novel characterization method of ions in liquid crystal materials by complex dielectric constant measurements. *Jpn J Appl Phys*. 1999;38(3R):1423–1427.
- [28] Karaawi AR, Gavriljak MV, Boronin VA, et al. Direct current electric conductivity of ferroelectric liquid crystals–gold nanoparticles dispersion measured with capacitive current technique. *Liq Cryst*. 2020;47(10):1507–1515.
- [29] Barbero G, Evangelista LR. Adsorption phenomena and anchoring energy in nematic liquid crystals. Boca Raton (FL): Taylor & Francis; 2006.
- [30] Inoue M. Review of various measurement methodologies of migration ion influence on LCD image quality and new measurement proposal beyond LCD materials. *J Soc Inf Disp*. 2020;28(1):92–110.
- [31] Mizusaki M, Ishihara S. A novel technique for determination of residual direct-current voltage of liquid crystal cells with vertical and in-plane electric fields. *Symmetry*. 2021;13:816.
- [32] Sasaki N. Nobuyoshi sasaki a new measurement method for ion density in TFT-LCD panels, molecular crystals and liquid crystals science and technology. Section A *Mol Cryst Liq Cryst*. 2001;367(1):671–679.
- [33] Dhara S, Madhusudana NV. Ionic contribution to the dielectric properties of a nematic liquid crystal in thin cells. *J Appl Phys*. 2001;90(7):3483–3488.
- [34] Kovalchuk OV. Adsorption of ions and thickness dependence of conductivity in liquid crystal. *Semicond Phys Quantum Electron Optoelectron*. 2011;14(4):452–455.
- [35] Kumar A, Varshney D, Prakash J. Role of ionic contribution in dielectric behaviour of a nematic liquid crystal with variable cell thickness. *J Mol Liq*. 2020;303:112520.
- [36] Shukla RK, Chaudhary A, Bubnov A, et al. Multiwalled carbon nanotubes-ferroelectric liquid crystal nanocomposites: effect of cell thickness and dopant

- concentration on electro-optic and dielectric behaviour. *Liq Cryst.* **2018**;45(11):1672–1681.
- [37] Garbovskiy Y. Ion capturing/ion releasing films and nanoparticles in liquid crystal devices. *Appl Phys Lett.* **2017**;110(4):041103.
- [38] Garbovskiy Y. Kinetics of ion-capturing/ion-releasing processes in liquid crystal devices utilizing contaminated nanoparticles and alignment films. *Nanomaterials.* **2018**;8(2):59.
- [39] Garbovskiy Y. Ions and size effects in nanoparticle/liquid crystal colloids sandwiched between two substrates. The case of two types of fully ionized species. *Chem Phys Lett.* **2017**;679:77–85.
- [40] Webb D, Garbovskiy Y. Overlooked ionic phenomena affecting the electrical conductivity of liquid crystals. *Eng Proc.* **2021**;11:1.
- [41] Mada H, Osajima K. Time response of a nematic liquid-crystal cell in a switched dc electric field. *J Appl Phys.* **1986**;60(9):3111–3113.
- [42] Takahashi S. The investigation of a dc induced transient optical 30-Hz element in twisted nematic liquid-crystal displays. *J Appl Phys.* **1991**;70(10):5346–5350.
- [43] Sugimura A, Zhong-Can OY. Dynamic behaviour of electric properties in a liquid crystal cell with polyimide boundaries. *Liq Cryst.* **1993**;14(2):539–544.
- [44] Ciuchi F, Mazzulla A, Pane A, et al. Ac and dc electro-optical response of planar aligned liquid crystal cells. *Appl Phys Lett.* **2007**;91(23):232902.
- [45] Palomares LO, Reyes JA, Barbero G. Optical response of a nematic sample submitted to a periodic external electric field: role of the ionic impurities. *Phys Lett A.* **2004**;333(1–2):157–163.
- [46] Macdonald JR. Impedance spectroscopy, emphasizing solid materials and systems. New York (NY): John Wiley & Sons; **1987**. p. 368.
- [47] Twarowski AJ, Albrecht AC. Depletion layer studies in organic films: low frequency capacitance measurements in polycrystalline tetracene. *J Chem Phys.* **1979**;70(5):2255–2261.
- [48] Koval'Chuk AV. Relaxation processes and charge transport across liquid crystals – electrode interface. *J Phys.* **2001**;13(24):10333–10345.
- [49] Senyuk BI, Smalyukh II, Lavrentovich OD. Switchable two-dimensional gratings based on field-induced layer undulations in cholesteric liquid crystals. *Opt Lett.* **2005**;30(4):349–351.
- [50] Shcherbinin DP, Konshina EA. Impact of titanium dioxide nanoparticles on purification and contamination of nematic liquid crystals. *Beilstein J Nanotechnol.* **2017**;8:2766–2770.
- [51] Yaroshchuk OV, Kiselev AD, Kravchuk RM. Liquid-crystal anchoring transitions on aligning substrates processed by a plasma beam. *Phys Rev E.* **2008**;77(3):031706.
- [52] Garbovskiy Y, Glushchenko A. Ferroelectric nanoparticles in liquid crystals: recent progress and current challenges. *Nanomaterials.* **2017**;7:361.
- [53] Garbovskiy Y, Emelyanenko AV, Glushchenko A. Inverse “guest–host” effect: ferroelectric nanoparticles mediated switching of nematic liquid crystals. *Nanoscale.* **2020**;12:16438–16442.
- [54] Lagerwall JPF, Scalia G, editors. Liquid crystals with nano and microparticles. Vol. 2. Singapore: World Scientific; **2016**. ISBN 9789814619257. ISBN 9789814619257
- [55] Dierking I. From colloids in liquid crystals to colloidal liquid crystals. *Liq Cryst.* **2019**;46(13–14):2057–2074.
- [56] Garbovskiy Y. Switching between purification and contamination regimes governed by the ionic purity of nanoparticles dispersed in liquid crystals. *Appl Phys Lett.* **2016**;108(12):121104.
- [57] Shukla RK, Liebig CM, Evans DR, et al. Electro-optical behaviour and dielectric dynamics of harvested ferroelectric LiNbO<sub>3</sub> nanoparticle-doped ferroelectric liquid crystal nanocolloids. *RSC Adv.* **2014**;4(36):18529–18536.
- [58] Basu R, Garvey A. Effects of ferroelectric nanoparticles on ion transport in a liquid crystal. *Appl Phys Lett.* **2014**;105(15):151905.
- [59] Garbovskiy Y, Glushchenko I. Ion trapping by means of ferroelectric nanoparticles, and the quantification of this process in liquid crystals. *Appl Phys Lett.* **2015**;107(4):041106.
- [60] Hsiao Y-C, Huang S-M, Yeh E-R, et al. Temperature dependent electrical and dielectric properties of nematic liquid crystals doped with ferroelectric particles. *Displays.* **2016**;44:61–65.
- [61] Lalik S, Deptuch A, Jaworska-Gołał T, et al. Modification of AFLC physical properties by doping with BaTiO<sub>3</sub> particles. *J Phys Chem B.* **2020**;124(28):6055–6073. DOI:10.1021/acs.jpcc.0c02401
- [62] Salah MB, Nasri R, Alharbi AN, et al. Thermotropic liquid crystal doped with ferroelectric nanoparticles: electrical behavior and ion trapping phenomenon. *J Mol Liq.* **2022**;357:119142.
- [63] Murakami S, Naito H. Electrode and interface polarizations in nematic liquid crystal cells. *Jpn J Appl Phys.* **1997**;36(4R):2222–2225.
- [64] Garbovskiy Y. Time-Dependent electrical properties of liquid crystal cells: unravelling the origin of ion generation. *Liq Cryst.* **2018**;45(10):1540–1548.
- [65] Furuichi K, Xu J, Inoue M, et al. Effect of ion trapping films on the electrooptic characteristics of polymer-stabilized ferroelectric liquid crystal display exhibiting V-shaped switching. *Jpn J Appl Phys.* **2003**;42(7R):4411–4415.
- [66] Huang Y, Bos PJ, Bhowmik A. The ion capturing effect of 5° SiO<sub>x</sub> alignment films in liquid crystal devices. *J Appl Phys.* **2010**;108(6):064502.